2016

Adaptive Beamsteering Cognitive Radar with Integrated Search-and-Track of Swarm Targets

Johnson, Z.W.; Romero, Ric

IEEE

IEEE Access
Multidisciplinary | Rapid Review | Open Access Journal

Digital Object Identifier

Adaptive Beamsteering Cognitive Radar with Integrated Search-and-Track of Swarm Targets

Z. W. JOHNSON, (Student, IEEE), R. ROMERO[1], (Senior Member, IEEE)
[1]Naval Postgraduate School, Monterey, CA 93940 USA (e-mail: rnromero@nps.edu)

ABSTRACT Adaptive beamsteering cognitive radar (AB-CRr) systems seek to improve detection and tracking performance by formulating a beam placement strategy adapted to their environment. AB-CRr builds a probabilistic model of the target environment that enables it to more efficiently employ its limited resources to locate and track targets. In this work, we investigate methods for adapting the AB-CRr framework to detect and track large target swarms. This is achieved by integrating the properties of correlated-motion swarms into both the radar tracking model and AB-CRr's underlying dynamic probability model. As a result, a list of newly CRr-integrated contributions are enumerated: a) improved uncertainty function design, b) incorporates Mahalanobis nearest neighbors multi-target association methodology into AB-CRr, c) introduces a novel Kalman-based consolidated swarm tracking methodology with a common velocity state vector that frames targets as a correlated collection of swarm members, d) introduces an improved uncertainty growth model for updating environment probability map, e) introduces a method for incorporating estimated swarm structure and behavior into the uncertainty update model referred to as "track hinting", and f) introduces new metrics for swarm search/detection and tracking called swarm centroid track error and swarm tracking dwell ratio. The results demonstrate that AB-CRr is capable of adapting its beamsteering strategy to efficiently perform resource balancing between target search and swarm tracking applications, while taking advantage of group structure and intra-swarm target correlation to resist large swarms overloading available resources.

INDEX TERMS cognitive radar, adaptive beamsteering, swarm tracking, swarm detection

I. INTRODUCTION

Unlike a traditional radar system, cognitive radar (CRr) employs a real-time transmit-receive feedback loop to adapt its resource allocation strategy to a dynamic target environment [1] [2] [3] [4]. As such, much of the activity for the last decade has been on adaptive transmit waveform design coupled with receive filter for CRr. Clearly, at this point, we cannot possibly list all the contributions in CRr waveform design but we listed a good sampling here for the interested reader [5] - [19] and these works contain several references. Additionally, a good introduction to the subject of CRr for target classification is [20] and plenty of references are listed there. Our interest in this paper however is not transmit waveform design nor classification. Our interest in this paper is the application of cognitive radar to adaptive beamsteering, in which a radar system develops a beam placement strategy based on prior measurements of the scene.

In applications where a radar system does not illuminate the entire search scene with a single beam for spatial resolution requirements, beam illumination of each region in the scene becomes a constrained resource in terms of temporal efficiency. Traditional beam rasterization schemes allocate an equal number of beam illuminations to each region in the search space, but depending on the application, this methodology can be far from optimal. Adaptive beamsteering cognitive radar can significantly improve both target search and tracking performance in scenarios where some prior information of the target environment is known [21] [22].

Adaptive beamsteering cognitive radar (AB-CRr) systems are well suited for applications where beamforming resources must be balanced between detection and tracking requirements [23] [24]. Prior art [25] introduces a weighted sum of target uncertainty in the scene and active track uncertainty via binary entropy. The work in [24] develops a parameterized cost function that similarly performs resource balancing between the resource competing applications. The

This article has been accepted for publication in a future issue of this journal, but has not been fully edited. Content may change prior to final publication. Citation information: DOI 10.1109/ACCESS.2021.3069350, IEEE Access

work in [26] introduces a third resource balancing methodology that modulates search versus tracking application resource allocation via uncertainty function design.

AB-CRr forms a probabilistic model of the radar channel [27]. This probabilistic model is leveraged to form a dynamic beamsteering strategy. As successive measurements of the target environment provide revision of the target probability model, the beamsteering strategy changes to match the new conditions. Both works in [25] and [28] present a framework for networked radar systems employing a cooperative beamsteering strategy. In comparison, our work in this paper investigates a single AB-CRr radar system with incomplete target state measurements (i.e. the single radar cannot directly measure target motion perpendicular to the receiver).

A methodology for selecting the next radar beam shape based on the underlying probability model is presented in [21]. This methodology relies on the information-theoretic binary entropy function to assign priority to regions of the probability model. In comparison, [26] introduces uncertainty functions as a generalized approach to translating the target probability model to a beamsteering strategy. The work in this paper extends upon [26] by investigating the impact of uncertainty functions on target tracking performance when integrated with Kalman filter tracking.

A novel and promising use case for adaptive beamsteering cognitive radar (AB-CRr) is swarm target detection and tracking. In this paper, we assume that swarm targets are distinguished from the more general multi-target case in that members of swarm share behavior characteristics (such as velocity). While a large number of targets can overwhelm traditional radar systems, a CRr can leverage probabilistic information about the search scene to improve performance in a saturated target environment. We note that tracking has a long history of contributions beyond Kalman including extended Kalman, particle filter theory, random matrix, Gaussian mixture and the like. It will be difficult to list all the contributions but we refer to recent works on advanced object tracking [29] - [34] and the related extended object tracking techniques cited in those articles. One possible issue with the use Mahalonobis (statistical) distance is it may be prone to erroneous target estimates, i.e. cardinality estimation [35] where some techniques like optimal sub-pattern assignment [36] may actually mitigate the issue.

This work makes the following contributions to the field of cognitive radar adaptive beamsteering:

- Develop a much improved uncertainty function that results in resource balancing behavior appropriate for the problem of swarm search/detection and tracking applications introduced in this paper
- Integrate a Mahalanobis nearest neighbors multi-target measurement association methodology with the AB-CRr architecture
- Introduces a novel Kalman-based consolidated swarm tracking methodology for AB-CRr with a common velocity state vector that frames targets as a correlated collection of swarm members, which results in new swarm state estimation techniques and associated multi-target tracking procedures
- Introduce an improved uncertainty growth model for updating the target environment probability map
- Introduce a method for incorporating estimated swarm structure and behavior into the uncertainty update model of the AB-CRr algorithm based on a collective swarm target model, referred to as "track hinting"
- Introduce quantitative and qualitative performance metrics for swarm target search/detection and tracking: swarm state estimation, swarm centroid track error, and swarm tracking dwell ratio

This work investigates the performance of an AB-CRr system in a simulated channel environment. Section II summarizes the channel and target environment model. Section III presents the adaptive beamsteering methodology employed in simulation. Section IV presents the swarm dynamics model. Section V presents the results of simulated radar performance with various swarm configurations. We summarize and conclude in section VI.

A. BOTTOM LINE UP FRONT (BLUF) RESULTS

A simulated video of our AB-CRr system in action searching, detecting, and ultimately tracking a ground-based swarm is shown here: https://youtu.be/hjcsKA2vtKg. The right panel shows adaptive beamsteering illumination of the scene while the left panel shows a swarm of target moving through the target scene as the AB-CRr system is used for detection and tracking.

II. CHANNEL MODEL

The adaptive beamsteering cognitive radar (AB-CRr) architecture investigated in this work employs a discrete search-space probabilistic model to describe its environment. For the benefit of the reader, some of the modeling concepts from [25] will be briefly reviewed presently.

Adaptive beamsteering cognitive radar can potentially be adapted to any radar system that employs steerable directional radar beams to probe a scene. An illustrative example is shown in Fig. 1, where the radar illuminator is assumed to be airborne, scanning the ground plane below it. Another example would simply be a stationary radar illuminating a large swath of ground or air space.

In both ground or airborne ground-search radar scenario, it is assumed that ground clutter is the dominant noise source. The radar system is also assumed to have an electronically steerable radar beam that can be controlled along two degrees of freedom: elevation and azimuth. When the radar beam is projected along the ground plane, this corresponds to Cartesian coordinates relative to the ground position of the airborne radar. Additionally, the radar system is able to measure Doppler frequency shift with the exception of tangential velocity when the beam is perpendicular to a target motion.

Further, it is assumed that there are multiple ground targets in the scene of interest moving in swarm formations. A

This article has been accepted for publication in a future issue of this journal, but has not been fully edited. Content may change prior to final publication. Citation information: DOI 10.1109/ACCESS.2021.3069350, IEEE Access

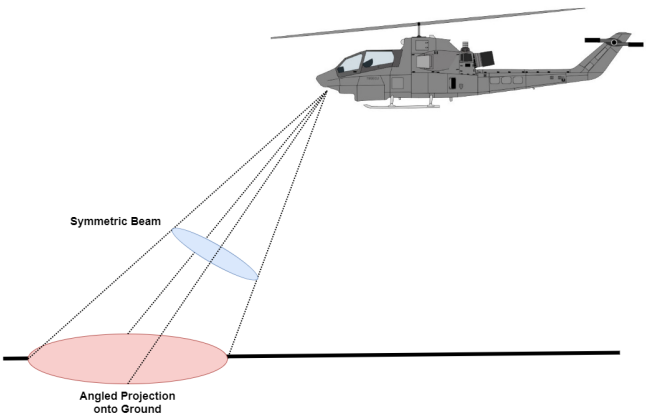

FIGURE 1. Scenario of operation: Airborne radar illuminating ground targets

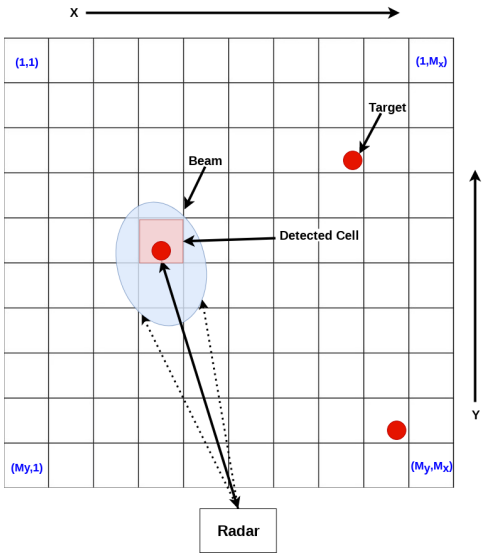

FIGURE 2. Azimuth-elevation angular measurements of a radar system projected onto a Cartesian plane

swarm formation is defined as a collection of targets with correlated motion and arbitrary, potentially dynamic, relative spatial orientation.

A. DISCRETE TARGET SPACE MODEL

The geometry considered is a 2-dimensional spatial region upon which the radar beam can be trained. Beam location in this 2-dimensional region from the polar coordinate system (elevation and azimuth) is easily translated to a discrete Cartesian grid representation (i.e. range and cross-range representation). The search space plane is divided into rectangular cells that each correspond to a subset of x-y measurements as depicted in Fig. 2. Each discrete cell in the grid has the Boolean attribute of "containing a target" or "not containing a target" within the continuous region of space it encloses.

The spatial search grid is composed of M_x cells and M_y cells corresponding to the azimuth and elevation angular cells of the search space. The Doppler shift is represented in the discrete grid by N_y Doppler cells. The resultant discrete

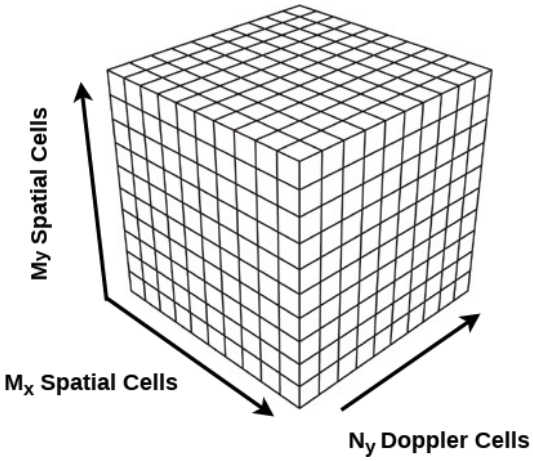

FIGURE 3. The search space is represented as a 3D matrix of Boolean values

search space is a matrix of size $\{M_x, M_y, N_y\}$, corresponding to x-axis position, y-axis position, and target velocity (Fig. 3).

B. RADAR CHANNEL MODEL

Referring to Fig. 2, the portion of the search space that is impinged upon by a radar beam at a given time is considered to be illuminated and the region not covered by the beam is considered to be unilluminated. The radar system measures the the amplitude of the backscatter from the illuminated region as well as its Doppler shift.

1) Phased Array Beamsteering

Phased array beamforming can be represented via a Kronecker product to produce a beamsteering matrix [25]

$$\mathbf{V} = \mathbf{a} \otimes \mathbf{b}_y \otimes \mathbf{c}, \tag{1}$$

where $\mathbf{a}$ and $\mathbf{c}$ are normalized spatial manifolds of the illuminated region and $\mathbf{b}_y$ is the temporal manifold that captures the discrete Doppler states of each spatial cell and are given by:

$$\begin{aligned} \mathbf{a} &= \frac{1}{\sqrt{M_x}} \exp\left(j2\pi k_x[0...M_x - 1]^T\right) \\ \mathbf{b}_y &= \frac{1}{\sqrt{N_y}} \exp\left(j2\pi d_y[0...N_y - 1]^T\right) \\ \mathbf{c} &= \frac{1}{\sqrt{M_y}} \exp\left(j2\pi k_y[0...M_y - 1]^T\right), \end{aligned} \tag{2}$$

where k_x and k_y are wave numbers, which are normalized (-0.5, 0.5) to correspond to the spatial region of the radar beam and d_y is the normalized range of Doppler frequencies [28].

Assuming that the power of beam energy is a constant value P_s along its aperture, the signal received from a beam illumination is represented by

$$\mathbf{s} = \sqrt{P_s}\mathbf{V}\mathbf{x} + \mathbf{n}, \tag{3}$$

This article has been accepted for publication in a future issue of this journal, but has not been fully edited. Content may change prior to final publication. Citation information: DOI 10.1109/ACCESS.2021.3069350, IEEE Access

where $\mathbf{s}$ is the received signal, $\mathbf{x}$ is a Boolean vector that represents the ground truth of true target locations in the cells illuminated by the beam, and $\mathbf{n}$ is noise. The vector $\mathbf{x}$ has a number of elements equal to the number of spatial cells illuminated by the beam multiplied by the number of discrete Doppler cells modelled in the discrete search space.

2) Environment Noise Model

Return measurement noise is the sum of both environmental noise e and receiver noise ω,

$$\mathbf{n} = e + \omega, \tag{4}$$

where e is modelled as zero-mean Gaussian with covariance $\mathbf{C}_\mathrm{e}$ and ω is zero-mean Gaussian with covariance matrix $\mathbf{C}_\omega$.

For simulation purposes, environmental clutter is initially modelled in the frequency domain [37]. In simulations for this work, the power spectral density (PSD) of environmental clutter is modelled by a Hamming window centered at zero frequency and spanning 0.67 of the normalized frequency range. Clutter return power is assumed to be 20 dB greater than thermal noise power for all JNR conditions investigated.

As is usual, the covariance of the thermal noise in the receiver is simply $\mathbf{C}_\omega = P_\omega \mathbf{I}$, where $\mathbf{I}$ is the identity matrix and thus the total clutter and noise covariance is given by

$$\mathbf{C}_n = \mathbf{C}_e + P_\omega \mathbf{I}. \tag{5}$$

C. TARGET SPACE PROBABILITY MODEL

Each discrete cell of the search space 3D matrix in Fig. 3 is assigned a probability of target presence, and each iteration of the beamsteering algorithm updates the probability of each cell according to both the return signal, prior cell probability, and underlying assumptions about the target environment.

1) Probability Update Methodology

a: Illuminated Region Update Method

This section summarizes the recursive Bayesian probability update methodology described in [26] and implemented in this AB-CRr framework. Current and past radar measurements of a discrete target state are used to recursively update the probability of target presence via Bayes Theorem [21],

$$P(H_i|\mathbf{z}_k) = \frac{P(H_i|\mathbf{z}_{k-1})p(\mathbf{z}_k|H_i)}{p(\mathbf{z}_k)}. \tag{6}$$

The sensor measurement $\mathbf{z}_k$ is for iteration or transmission k. Hypothesis H_i is a member of the set of possible permutations of targets in the cells under illumination. Assuming that a maximum of one target is present in each cell, then there are 2^M such hypothesis permutations, where M is the total number of cells illuminated by the radar beam. M is equivalent to the number of spatial cells encompassed by the radar beam multiplied by the number of Doppler frequency cells in the scene.

Thus each return measurement hypothesis can be formed as

$$\begin{aligned} H_0 &: \mathbf{z} = \mathbf{n} \\ H_1 &: \mathbf{z} = \mathbf{s}_1 + \mathbf{n} \\ H_2 &: \mathbf{z} = \mathbf{s}_2 + \mathbf{n} \\ H_3 &: \mathbf{z} = \mathbf{s}_1 + \mathbf{s}_2 + \mathbf{n} \\ &\vdots \\ H_{2^M-1} &: \mathbf{z} = \mathbf{s}_1 + \mathbf{s}_2 + ... + \mathbf{s}_M + \mathbf{n}, \end{aligned} \tag{7}$$

where $\mathbf{s}_i$ is the return signal anticipated from the i^{th} cell illuminated by the beam. The number of permutations grows exponentially with the number of target state cells encompassed by the beam. If the number of targets that can appear in the illuminated region is limited to r, however, then the number of hypotheses that must be computed is reduced to [27]

$$N = \sum_{k=0}^{r} \binom{M}{k}. \tag{8}$$

Note that when the maximum number of targets r is equal to M (the total number of cells illuminated by the beam), Eq. (8) becomes a special case of the binomial series [38],

$$N = \sum_{k=0}^{M} \binom{M}{k} = \sum_{k=0}^{M} \binom{M}{k} 1^k = 2^M, \tag{9}$$

and the total number of possible permutations matches the number listed in Eq. (7).

Considering that received signal $\mathbf{z}_k$ is a jointly Gaussian noisy signal with covariance matrix $\mathbf{C}_\mathbf{z}$, the conditional joint probability distribution is given by

$$p(\mathbf{z_k}|H_i) = \frac{1}{\pi^l |\mathbf{C_z}|} \exp{(\mathbf{s}_i - \mathbf{z}_k)^H \mathbf{C}_\mathbf{z}^{-1} (\mathbf{s}_i - \mathbf{z}_k)}, \tag{10}$$

where l is the number of elements in the received signal vector $\mathbf{z}_k$. The prior probability of a target hypothesis can be computed from cell target probabilities via

$$P(\mathbf{z}_{k-1}|H_i) = \prod_{c=1}^{M} (P_{c,k-1})^{b_c} (1 - P_{c,k-1})^{1-b_c}, \tag{11}$$

where b_c is either 1 or 0 corresponding to whether hypothesis H_i includes a target present in cell c. $P(\mathbf{z}_k|H_i)$ and $P(\mathbf{z}_k)$ do not have to be directly computed, rather, the ratio of the two values can be computed via

$$\frac{P(\mathbf{z}_k|H_i)}{P(\mathbf{z}_k)} = K^{-1} \exp{(\mathbf{s}_i - \mathbf{z}_k)^H \mathbf{C}_\mathbf{z}^{-1} (\mathbf{s}_i - \mathbf{z}_k)}, \tag{12}$$

where K is a normalization factor equal to the sum of each hypothesis joint probability:

$$K = P(\mathbf{z}_k) = \sum_{i=0}^{2^M-1} P(\mathbf{z}_k|H_i). \tag{13}$$

This article has been accepted for publication in a future issue of this journal, but has not been fully edited. Content may change prior to final publication. Citation information: DOI 10.1109/ACCESS.2021.3069350, IEEE Access

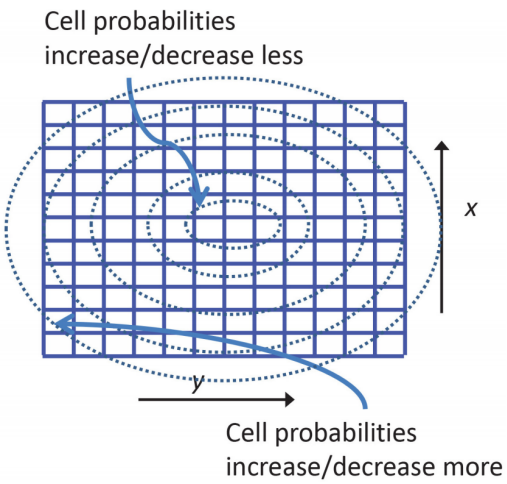

FIGURE 4. Non-uniform uncertainty growth model. Source: [25].

The updated cell probabilities can be computed by summing each hypothesis that includes a target present in the cell c,

$$P = \sum_{c=1}^{M} b_c P(\mathbf{z}_k|H_i). \tag{14}$$

b: Unilluminated Region Update Method

With each illumination of the radar system, time elapses and the majority of cells in the search grid are not illuminated. Therefore, the uncertainty of these unilluminated cells grows during the period of non-observation. As the system progresses through iterations, the uncertainty of unilluminated cells grows until the adaptive beamsteering algorithm illuminates that cell and updates its corresponding uncertainty value.

One of the greatest advantages of a cognitive radar approach towards search optimization is that prior knowledge of the target environment can be readily integrated into the scenario, impacting the beamsteering behavior of the radar accordingly. In a simple radar search scenario, for example, it may be reasonable to assume that targets are most likely to enter into the search space from the edges of the grid. Translated into terms of search grid uncertainty: with each successive time step, the chance that a target appears or disappears from the edges of the map is greater than anywhere else, as was utilized in [25] as shown here in Fig. 4 for the benefit of the reader. This assumption about target behavior can be integrated into the cognitive radar probability model by implementing non-uniform uncertainty growth across the probability cells of the search grid. For example, the uncertainty increment value used on a given cell can be defined in relation to the Euclidean distance of spatial position of a cell to the center of the search grid.

c: Improved Update Methodology

One problem with this methodology is that there is no uncertainty growth at the center of the search grid and thus can be restrictive. To overcome these limitations and greatly improve upon this model, a generalized probability update increment is introduced in this work:

$$\Delta U_{i,j,k} = \alpha \left(1 + \sqrt{2}\beta\, d(i,j)\right), \tag{15}$$

where $\Delta U_{i,j,k}$ is the uncertainty increment for a given cell, α is a coefficient that defines the overall rate of uncertainty growth, and β relates the relative significance of Euclidean distance from the center of the search space to the baseline growth rate. The distance of a discrete cell from the center of the search space is given by the equation $d(i,j)$:

$$d(i,j) = \sqrt{\left(i - \frac{M_x - 1}{2}\right)^2 + \left(j - \frac{M_y - 1}{2}\right)^2} \tag{16}$$

Because the normalized spatial ranges of the search scene are (-0.5, 0.5), the maximum normalized distance from the center is $0.5\sqrt{2}$. When $\beta = 0$, uncertainty growth is uniform across all cells. When $\beta >> 1$, uncertainty growth behaves as described in Fig. 4.

2) Probability Map Initialization

There are multiple possible models for how to initialize the 3-dimensional probability map of the cognitive radar system. One initialization technique is to assume that no targets exist in the search space at the onset of operation. There is a problem with this approach. The approach initializes the scene with zero uncertainty across the search space and leaves the cognitive radar beam selection algorithm to initially illuminate at some arbitrary beam area. Although the probabilities will increase at the unilluminated areas, they may not translate to high uncertainty and such areas may be left unilluminated until probabilities reach favorable uncertainty values.

A second option is to assume that a finite number of targets already exist in the search space, and distribute the cell probabilities uniformly based on this assumption. For example, if one target is assumed to be present in the search area and there are 100 cells, each cell might be assigned an initial probability of 0.01, such that the sum of all the cells equals 1, as suggested in [21]. If some prior knowledge of the environment is assumed, then it can be applied to provide greater initial probability to cells that are known to be more likely to initially contain a target (such as the edges of a map). However, if the number of cells is truly significant then the initial probability will be very low, which may not be practical for a given target scenario.

A third option is to arbitrarily initialize the probability of each cell to 0.5 if the entropy function is used as suggested in [25]. As a result, at the start of operation, the cognitive radar assigns a high uncertainty value to each unilluminated cell. As such, the initial behavior of the system is biased towards illuminating each cell at least once before settling into some kind of steady state search behavior. The utility of this approach is that it can easily be modified for different

This article has been accepted for publication in a future issue of this journal, but has not been fully edited. Content may change prior to final publication. Citation information: DOI 10.1109/ACCESS.2021.3069350, IEEE Access

uncertainty functions by placing the probability corresponding to the highest uncertainty in each cell as we preliminary illustrated in [26]. Because of the impractical issues of the first two initialization methods, in this implementation, the third option is selected. It is also desirable that every cell in the search scene is illuminated at the onset of the simulation run to identify any targets already in the scene. This approach is named the uncertainty function-based (UFB) probability map initialization. Unlike the purely entropy-based function, this approach can accommodate any uncertainty function.

III. ADAPTIVE BEAMSTEERING COGNITIVE RADAR

The cognitive radar system employs the probability model translated to an uncertainty map to iteratively select its next beam placement, which in turn drives future beamsteering behavior.

A. UNCERTAINTY MAPPING OF PROBABILITY MODEL

In order for the 3-dimensional probability model to be employed in a beam selection strategy, probability values are mapped to uncertainty values. In [25], a binary entropy function is used which maps 0.5 to have the maximum uncertainty and beam priority is placed on cells around this probability. However, such action can actually impede detection of cells containing targets where probabilities are already close to some required threshold. In [26], we proposed uncertainty to be a cost metric which describes the significance of a given cell probability to the cognitive radar overall assessment of performance (i.e. some probability threshold for detection). The adaptive beamsteering algorithm seeks to minimize the cumulative uncertainty metric of the entire scene model, so the selection of an uncertainty metric drives the overarching behavior of the cognitive radar beamsteering strategy.

1) Uncertainty Metric

The 3-dimensional matrix is composed of probabilities ranging from 0 to 1, where 1 is a 100% probability of target presence in a cell. An uncertainty function maps probability values to uncertainty values between 0 and 1. An uncertainty value of 0 contributes no cost to the cumulative uncertainty of the system, while an uncertainty value of 1 is the maximum contribution a cell can contribute.

2) The Need for Better Uncertainty Function Design

Provided that a AB-CRr beamsteering strategy seeks to minimize the cumulative uncertainty of the search scene over time, a series of inferences can be made about the impact of an uncertainty function on the resultant beamsteering strategy.

First, the beam selection algorithm will orient its next beam at the spatial region associated with the highest contribution of uncertainty. It is intuitive that illuminating the beam area with the highest cumulative uncertainty will reduce the overall uncertainty of the scene during that observation. Of course, a well formed uncertainty function should output an uncertainty of 0 at input probabilities 0 and 1. This is satisfied by the binary entropy function, but may not necessarily be optimal for the search function.

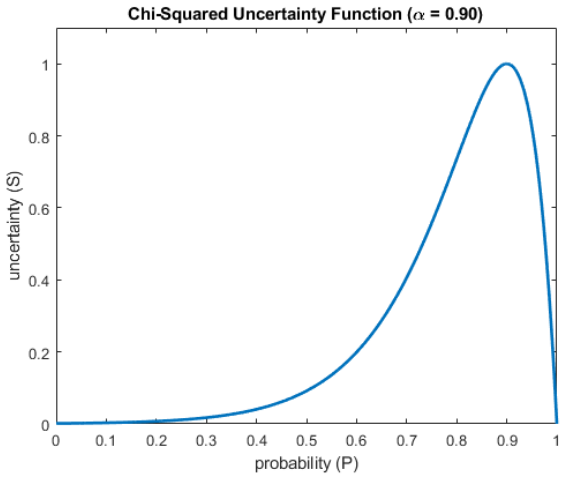

FIGURE 5. Chi-squared uncertainty function

Second, if illuminating a cell results in an increase in the corresponding uncertainty value for the cell, the beam selection algorithm will continue to illuminate that cell until the uncertainty begins to drop. This observation assumes that the cell in question is illuminated because its region contributed the most uncertainty in the scene and that the unilluminated region uncertainty growth is much slower than the illuminated region uncertainty change. As a consequence, the beam selection algorithm can be expected to continue to illuminate a cell as long as the derivative of the uncertainty function at its instantaneous probability value is positive. Therefore, if the desired beam selection behavior is to continue to illuminate an uncertain true-target cell until a threshold probability for decision is reached, then the global maximum of the uncertainty function should be placed at or near the desired or required probability of detection.

Prior art [25] used the binary entropy function in the role of an uncertainty function, while this meets the criterion of an uncertainty function as it is described above, the binary entropy function has a maximum value at $P = 0.5$. In practice, this results in beamsteering behavior that illuminates potential targets until it reaches a 50% probability of target presence and then moves to a different region without further investigation. Instead, a Chi-squared inspired uncertainty function is selected for its balanced performance with integrated search and track applications based on results from our preliminary work in [26]:

$$S(P) = \begin{cases} 0 & P = 0 \\ \frac{1-P}{1-\alpha}\exp\left(\frac{P-\alpha}{1-\alpha},\right) & P \neq 0 \end{cases}. \tag{17}$$

Equation 17 is a reversed Chi-squared distribution with 4 degrees of freedom scaled to a maximum value of one. The variable α indicates the probability value at which the uncertainty function has its local maximum. Figure 5 shows the Chi-squared uncertainty function with $\alpha = 0.90$.

This article has been accepted for publication in a future issue of this journal, but has not been fully edited. Content may change prior to final publication. Citation information: DOI 10.1109/ACCESS.2021.3069350, IEEE Access

3) Target Scene to Beamsteering Scene Mapping

Upon transforming the target probability matrix into uncertainty values, the next beam location is selected by locating the beam position that encompasses the greatest cumulative amount of cell uncertainty. Note that the uncertainty matrix U has dimensions $M_x \times M_y \times N_y$ while the beamsteering search plane has dimensions $M_x \times M_y$. The uncertainty matrix can be projected to $M_x \times M_y$ by computing the mean uncertainty value of Doppler cells at each spatial index of U. Thus the 2-dimensional uncertainty matrix is given by,

$$Q_{j,k} = \frac{1}{N_y} \sum_{l=0}^{N_y-1} U_{j,k,l}, \tag{18}$$

where Q is the $M_x \times M_y$ projection of U, N_y is the number of Doppler cells over which the mean is taken, and l is the Doppler cell index.

B. ADAPTIVE BEAMSTEERING OPTIMIZATION

A cognitive radar beamsteering strategy will seek to minimize the cumulative value of the matrix Q. A simple methodology for minimizing the cumulative value of Q is to select a beam at each iteration of radar illumination that is anticipated to reduce the cumulative uncertainty more than any other beam configuration. It is assumed that the cognitive radar operates at a reasonable SNR such that the uncertainty of any cell illuminated by the radar beam is reduced. Then, the condition for the optimal next beam is

$$(U_{k+1}|B_k^*) \geq (U_{k+1}|B_k), \tag{19}$$

where k is the illuminating iteration number, B^* is the optimal beam selection and B is the set of all possible beam configurations in the search scene.

If the shape of the beam is assumed to be rectangular and smaller than the search scene, then the optimal next beam can be easily found via a 2-dimensional convolution $(**)$:

$$< i, j >_{B^*} = \arg\max_{i,j} \tilde{B} ** Q, \tag{20}$$

where $< i, j >$ are the x and y discrete cell indices of the lower corner of the optimal beam, $\tilde{B}$ is a matrix of ones with the dimensions of the radar beam, and Q is the spatial uncertainty matrix.

IV. SWARM DYNAMICS AND TRACKING

The AB-CRr system uses a Kalman filter to track a detected target or target swarm through the search scene. The Kalman filter estimates the constant motion state of a target and is represented by the state vector

$$\hat{\mathbf{x}} = \begin{bmatrix} x \\ v_x \\ y \\ v_y \end{bmatrix}. \tag{21}$$

Target measurements by the cognitive radar are discrete space, while the Kalman filter estimates the target space in continuous space. This is accounted for in the design of Kalman filter parameters.

A. INITIALIZING KALMAN MODEL

The Kalman filter is initialized by the first measurement of a detected cell. Estimate covariance and measurement covariance are approximated to account for the error incurred by discrete measurements of the target state. In this section, variables $\mathbf{Q}$ and $\mathbf{K}$ have different meanings than the same variable names discussed previously and pertain specifically to the development of the Kalman filter.

1) Initial State

A target is said to be "detected" when a cell of the search space exceeds a threshold probability of target presence. In the single target case, the first cell to reach this target probability immediately after illumination by a beam is used to initialize the target state estimate. Each cell in the search scene corresponds to a measurement $\hat{\mathbf{z}}$, which represents the measured target state at the center of the discrete region. As the search scene has three dimensions, the detected target cell map measurement of continuous space-related parameters is given by

$$\hat{\mathbf{z}} = \begin{bmatrix} x \\ y \\ v_y \end{bmatrix}. \tag{22}$$

As the initial measurement contains no information about the x-axis velocity of the detected target, it is initially assumed to be zero and the target state estimate is initialized as

$$\hat{\mathbf{x}}_i = \begin{bmatrix} x_i \\ 0 \\ y_i \\ v_{y_i} \end{bmatrix}. \tag{23}$$

2) Measurement Covariance

The dominant factor in measurement error is assumed to be quantization error of the search space. If the x-axis of the search space has a normalized range of $(-0.5, 0.5)$ and there are N discrete values that are evenly spaced, then each discrete cell encloses a continuous range of normalized values $\frac{1}{N}$ wide. Given that a target exists within a detected cell, the probability of the true target parameter in this range is uniformly distributed. However, the Kalman filter assumes that the measurement noise is normally distributed. As an approximation, the standard deviation of each measurement axis is said to be equal to the quantization error of the discrete model. Each axis is said to be independent of the other axis, yielding a measurement covariance matrix

$$R = \begin{bmatrix} \frac{1}{M_x^2} & 0 & 0 \\ 0 & \frac{1}{M_y^2} & 0 \\ 0 & 0 & \frac{1}{N_y^2} \end{bmatrix}. \tag{24}$$

This article has been accepted for publication in a future issue of this journal, but has not been fully edited. Content may change prior to final publication. Citation information: DOI 10.1109/ACCESS.2021.3069350, IEEE Access

3) Target Covariance

The target is assumed to be maneuvering with a stochastic motion model. Only constant motion is modelled in the target state, but acceleration is modelled with white Gaussian variance in the target velocity. This is represented with the target state covariance matrix

$$Q = \begin{bmatrix} 0 & 0 & 0 & 0 \\ 0 & \sigma_a^2 & 0 & 0 \\ 0 & 0 & 0 & 0 \\ 0 & 0 & 0 & \sigma_a^2 \end{bmatrix}. \tag{25}$$

4) State Estimate Covariance

The initial state estimate covariance is initialized as

$$P = \begin{bmatrix} \frac{1}{M_x^2} & 0 & 0 & 0 \\ 0 & 1 & 0 & 0 \\ 0 & 0 & \frac{1}{M_y^2} & 0 \\ 0 & 0 & 0 & \frac{1}{N_y^2} \end{bmatrix}. \tag{26}$$

Given that x-axis velocity can range from -0.5 to 0.5 in the normalized range, the normal approximation variance of x-axis measurement is therefore initialized with a value of 1.

5) Track Update

Using the probabilistic model, a target detection is defined as any cell whose target probability crosses above the detection threshold in a given illumination iteration. In the single target case, it is assumed that every target detection associates with the active target track. Therefore, for every iteration of beam selection with a valid target detection, the standard Kalman update procedure is applied with a constant observation matrix

$$H = \begin{bmatrix} 1 & 0 & 0 & 0 \\ 0 & 0 & 1 & 0 \\ 0 & 0 & 0 & 1 \end{bmatrix}. \tag{27}$$

In the case where there is no target detection over one radar illumination cycle, the observation matrix is null, and only state vector and estimate covariance prediction are performed.

B. MULTI-TARGET TRACK ASSOCIATION

The most direct approach to multiple target tracking is to assign each target in the scene its own Kalman track file. To accomplish this, detected target measurements must be associated with their corresponding tracks at each measurement interval.

1) Nearest Neighbors Measurement Association

When a target is detected, it is first tested against each existing target track in the swarm model via a Chi-squared test. The Mahalanobis distance between each track in the beam scene and each target detection is computed via:

$$d_i = (\mathbf{z}_k - H\hat{\mathbf{x}}_k)^T (R + H_i P_{k|k-1} H_i^T)^{-1} (\mathbf{z}_k - H\hat{\mathbf{x}}_k) \tag{28}$$

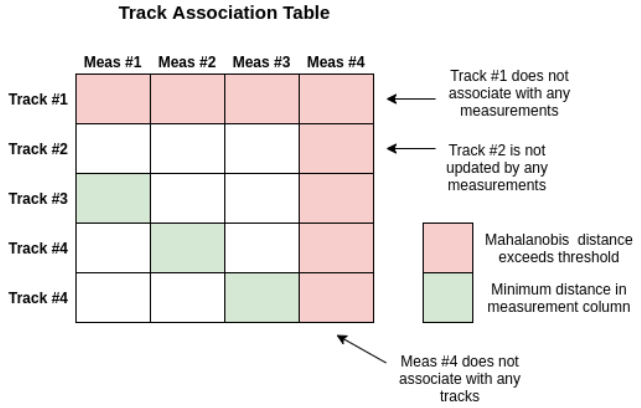

FIGURE 6. Track-to-measurement association table (Mahalanobis nearest neighbors method)

where d_i is the Mahalanobis distance between detected target and track i, H_i is the observation matrix that corresponds to that association, and $\mathbf{z}_k$ is the measurement vector.

For improved computational efficiency given that measurement covariance R is constant across iterations, the Woodbury matrix identity is preferable, yielding:

$$\begin{aligned} \mathbf{y}_k &= \mathbf{z}_k - H\hat{\mathbf{x}}_k \\ d_i &= \mathbf{y}_k^T R^{-1} \mathbf{y}_k - \mathbf{y}_k^T R^{-1} H_i (P_{k|k-1} \\ &\quad + H_i^T R^{-1} H_i)^{-1} H_i R^{-1} \mathbf{y}_k. \end{aligned} \tag{29}$$

The detected target is then associated with the target track with the smallest Mahalanobis distance from itself. If each track exceeds a threshold Chi-squared association value (not to be confused with and unrelated to the Chi-squared inspired uncertainty function previously introduced), then the detected target is assumed to be a new (previously unobserved) target and is added to the swarm model.

2) Multiple Measurements Nearest Neighbors Association

In the event that multiple targets are detected in a single beam illumination, the nearest neighbors model is easily extended to manage track associations. First, an association table is generated for all measurements and target tracks (Fig. 6). Next, each target detection is compared against candidate target tracks. If one or more target tracks meet the Chi-squared criterion for association, the nearest target track is updated with that target measurement. If none of the tracks associate with a detection, this detection is considered a new target. If a target track is illuminated by the beam but does not associate with any measurements, it is assumed to be a deprecated track and is removed from the swarm model. This target association and management algorithm is summarized in Fig. 7.

C. CONSOLIDATED SWARM KALMAN TRACKING

The Kalman tracking problem for correlated velocity swarm targets can be simplified by assuming that all the members of a swarm have the same mean velocity such that the

This article has been accepted for publication in a future issue of this journal, but has not been fully edited. Content may change prior to final publication. Citation information: DOI 10.1109/ACCESS.2021.3069350, IEEE Access

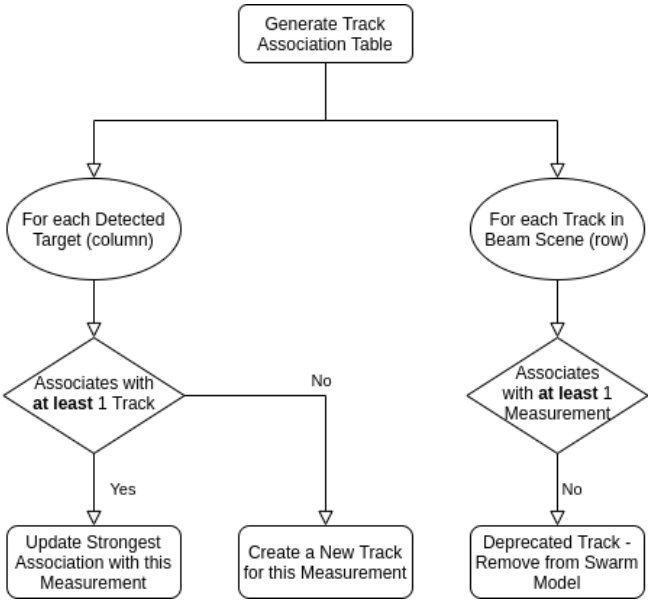

FIGURE 7. Track-to-measurment association flow diagram

swarm formation is maintained. When this is the case, each target track can be represented in a single state vector. Each observation of a target in the swarm updates the velocity state estimate of the entire swarm, increasing the number of velocity measurements for the Kalman tracker. The new state model for a two target swarm can be expressed as:

$$\hat{\mathbf{x}} = \begin{bmatrix} \bar{v}_x \\ \bar{v}_y \\ x_1 \\ y_1 \\ x_2 \\ y_2 \end{bmatrix} \tag{30}$$

Note that instead of tracking each target separately, all of the member targets of a swarm are represented in a single state vector. The transition matrix for the consolidated swarm state vector is given as:

$$F = \begin{bmatrix} 1 & 0 & 0 & 0 & 0 & 0 \\ 0 & 1 & 0 & 0 & 0 & 0 \\ \Delta & 0 & 1 & 0 & 0 & 0 \\ 0 & \Delta & 0 & 1 & 0 & 0 \\ \Delta & 0 & 0 & 0 & 1 & 0 \\ 0 & \Delta & 0 & 0 & 0 & 1 \end{bmatrix} \tag{31}$$

where Δ is the time step between iterations. Future values of the state estimate vector can be computed at discrete times $t = \tilde{n}\Delta$ via:

$$\hat{\mathbf{x}}[\tilde{N} + \tilde{n}] = F^{\tilde{n}}\hat{\mathbf{x}}[\tilde{N}]. \tag{32}$$

where $\tilde{n}$ is the discrete time index.

Because the radar system is limited to only measuring targets enclosed within its beam for a given iteration, the system will not always measure each member of a swarm in a single iteration. Therefore, the observation matrix changes with each iteration of measurement. If no targets are measured by a beam illumination, the observation matrix is null and no Kalman update occurs. If the first target member of a swarm is detected in a beam illumination, then the observation matrix is formed:

$$H_{1,0} = \begin{bmatrix} 1 & 0 & 0 & 0 & 0 & 0 \\ 0 & 0 & 1 & 0 & 0 & 0 \\ 0 & 0 & 0 & 1 & 0 & 0 \end{bmatrix} \tag{33}$$

Similarly, if the second member of a swarm track is detected, the observation matrix is formed:

$$H_{0,1} = \begin{bmatrix} 1 & 0 & 0 & 0 & 0 & 0 \\ 0 & 0 & 0 & 0 & 1 & 0 \\ 0 & 0 & 0 & 0 & 0 & 1 \end{bmatrix} \tag{34}$$

Here $H_{1,0}$ corresponds to the case where only the first target associates, while $H_{0,1}$ corresponds to the case where only the second target associates with the measurement. If multiple targets are observed in a single beam, the update procedure is performed multiple times, once for each associated track in the swarm.

The subsequent Kalman update procedure for each iteration updates the state estimate of each target in the swarm even if only one of the targets is directly observed via

$$\begin{aligned} K &= P_{k+1|k}H_k^T(H_kP_{k+1|k}H_k^T + R_k) \\ P_{k+1|k+1} &= (I - KH_k)P_{k+1|k} \\ \hat{\mathbf{x}}_{k+1|k+1} &= \hat{\mathbf{x}}_{k+1|k} + K(\mathbf{z}_k - H_k\hat{\mathbf{x}}_k) \end{aligned} \tag{35}$$

where $\mathbf{K}$ is the Kalman gain matrix, $\mathbf{P}$ is the state estimate covariance matrix, and k is the iteration index of the Kalman filter.

D. ASSOCIATING TARGETS TO CONSOLIDATED TRACK

Measurement-to-track association for a consolidated swarm track follows the same procedure as the multiple track file method presented previously. The only modification for the consolidated tracking system is that the observation matrix H_i in Eq. (29) becomes the consolidated state vector observation matrix corresponding to its associated track ($H_{0,1}$, $H_{1,0}$, etc.).

E. INITIALIZING AND REMOVING TARGETS FROM THE SWARM MODEL

1) Initializing Newly Detected Targets

In our implementation, if the Mahalanobis distance between a measurement and each active track exceeds the 95% Chi squared association test, it is assumed to be a newly observed target. New target tracks are appended to the existing consolidated state estimate and estimate covariance matrix. The state vector is updated with the measured spatial coordinates of the new target:

This article has been accepted for publication in a future issue of this journal, but has not been fully edited. Content may change prior to final publication. Citation information: DOI 10.1109/ACCESS.2021.3069350, IEEE Access

$$\hat{\mathbf{x}}_{k+1|k} = \begin{bmatrix} \hat{\mathbf{x}}_{k|k} \\ \mathbf{z}_{x,k} \\ \mathbf{z}_{y,k} \end{bmatrix} \tag{36}$$

and the estimate covariance matrix is updated with the spatial covariance sub-matrix of the associated measurement:

$$P_{k+1|k} = \begin{bmatrix} P_{k|k} & 0 & 0 \\ 0 & \frac{1}{M_x^2} & 0 \\ 0 & 0 & \frac{1}{M_y^2} \end{bmatrix}. \tag{37}$$

2) Removing Dead Tracks

A mechanism for removing old or inaccurate target tracks is also necessary for dense swarm formations. In this work, if the position of an active target track is illuminated by a beam and fails to associate at a 99% level with any of the subsequent detection measurements, it is presumed to be a bad track and is marked for removal. The procedure for removing the first target from a two-target consolidated track begins by forming a selection matrix for the spatial sub-matrix of the first target:

$$Y = \begin{bmatrix} I_2 & 0 & 0 \\ 0 & 0 & I_2 \end{bmatrix} \tag{38}$$

.

where $\mathbf{I}_2$ is the 2-by-2 identity matrix. The state matrix is then updated via:

$$\hat{\mathbf{x}}_{k+1|k} = Y\hat{\mathbf{x}}_{k|k} \tag{39}$$

and the estimate covariance matrix is updated with:

$$P_{k+1|k} = Y^T P_{k|k} Y. \tag{40}$$

Note that the swarm velocity estimate is unaffected by the removal of a target track. The swarm velocity estimate is assumed to converge to the mean velocity of all of the targets in the consolidated tracking model.

F. SWARM STATE ESTIMATION

When considering targets as members of a swarm, it is often more useful to describe characteristics of the swarm in aggregate, rather than the characteristics of each of its component parts. In this section, methods of describing the state and behavior of swarms are discussed. These metrics will serve as the basis of performance estimation for swarm detection and tracking in the following chapter.

1) Swarm Centroid Estimate

The centroid of a point cloud is defined as the mean value along each coordinate axis. For the individual target track methodology, the centroid of the swarm is defined as

$$\hat{\mathbf{x}}_c = \frac{1}{N_{tgt}} \sum_{n=1}^{N_{tgt}} \hat{\mathbf{x}}_n, \tag{41}$$

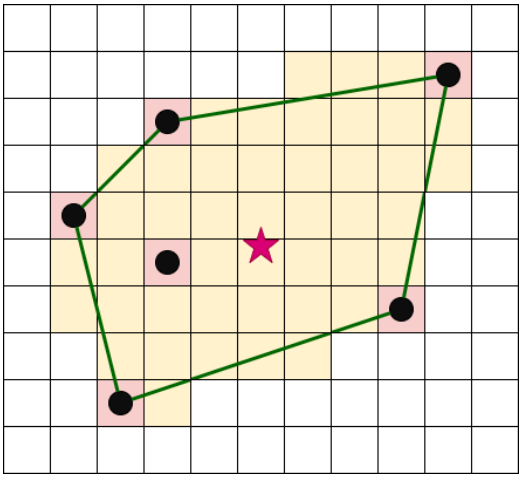

FIGURE 8. Swarm region estimate in discrete space

where $\hat{\mathbf{x}}_c$ is the state vector of the swarm centroid estimate, $\hat{\mathbf{x}}_n$ is the state vector of the n^{th} track, and N_{tgt} is the total number of target tracks in the swarm model. For the consolidated swarm tracking model, the centroid estimate is similarly computed as

$$\hat{\mathbf{x}}_c = \begin{bmatrix} 0 & 0 & \frac{1}{N_{tgt}} & 0 & \frac{1}{N_{tgt}} & 0 & \dots \\ 1 & 0 & 0 & 0 & 0 & 0 & \dots \\ 0 & 0 & 0 & \frac{1}{N_{tgt}} & 0 & \frac{1}{N_{tgt}} & \dots \\ 0 & 1 & 0 & 0 & 0 & 0 & \dots \end{bmatrix} \hat{\mathbf{x}} \tag{42}$$

where $\hat{\mathbf{x}}$ is the consolidated swarm state vector.

G. SWARM SPATIAL REGION ESTIMATE

In some cases, it may be useful to estimate the region of space that a target swarm resides in. This can be achieved by forming a polygon that encapsulates each target track in the swarm model. First, regarding the swarm as a point cloud of spatial coordinates, we solve the convex hull problem to generate the boundary points of a polygon [39]. This polygon is subsequently discretized back into the probability model grid to form a subset of probability cells in which the swarm is said to reside. Fig. 8 is a 2-dimensional visualization of this process, where black points are the continuous state estimates of swarm targets, the dark green polygon is the convex hull of the target point cloud, and yellow cells are the discrete cells of the probability model that are said to be members of the swarm region. The red star corresponds to the spatial centroid of the target swarm. As implied in Fig. 8, we assume that cells are configured such that one target occupies one cell at a time.

H. ADAPTIVE BEAMSTEERING TRACK FEEDBACK

As in the single target case, multi-target track information can be used as feedback into the uncertainty model that drives adaptive beamsteering. There are numerous possible feedback models that can be employed, but in this work, the uncertainty of the swarm estimate region naturally grows

This article has been accepted for publication in a future issue of this journal, but has not been fully edited. Content may change prior to final publication. Citation information: DOI 10.1109/ACCESS.2021.3069350, IEEE Access

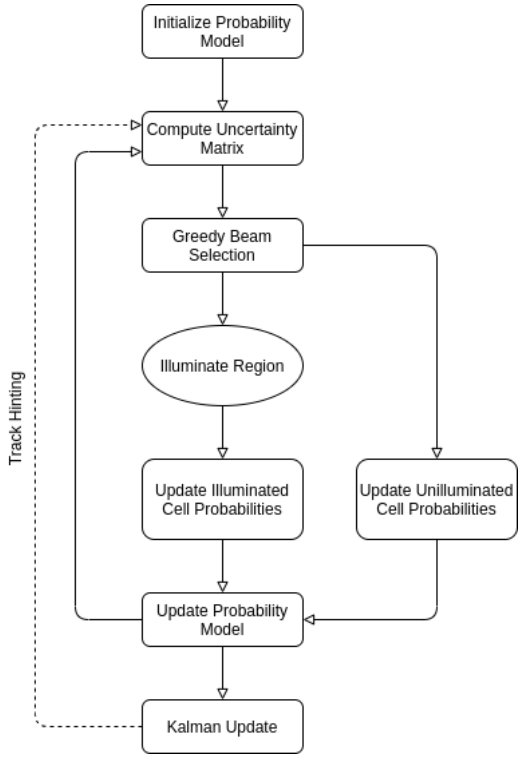

FIGURE 9. Adaptive beamsteering cognitive radar algorithm

with each time interval (iteration). As a result, adaptive beamsteering behavior is induced in such a way that not only increases dwell time on known swarm targets, but allocates more beam time to the detection and tracking of potential interior members of the target swarm.

The target track state estimate can be used as feedback into the adaptive beamsteering uncertainty model in order to improve tracking performance. After updating the probability map (3-D matrix) following a beam illumination and computing its associated uncertainty matrix, a small uncertainty value γ is incremented to the cell corresponding to the target state estimate. Over numerous iterations, the uncertainty value of the cell associated with the estimated state of the target ($\hat{\mathbf{x}}$) grows faster than the rest of the map and causes the adaptive beamsteering algorithm to illuminate the estimated position, effectively verifying the estimate of the Kalman filter with an observation. In this way, track hinting (in Figure 9) can inject prioritization to target tracking into the adaptive beamsteering algorithm. Fig. 9 illustrates the integration of track feedback into the AB-CRr framework.

Extending AB-CRr target detection and tracking to multiple targets can be achieved by introducing a Kalman track file for each newly detected target. However, as the number of targets in the scene grows large, the tracking resources of a cognitive radar, like a traditional radar system, will become overwhelmed, lacking the resources to maintain each individual target track. Consolidated state vector Kalman tracking promises better performance with large target swarms, provided that the swarm targets move in a cooperative fashion (e.g. correlated velocity). This significant benefit will be illustrated in the next section.

V. SIMULATION AND PERFORMANCE

The integrated search-and-track performance of an AB-CRr system is modelled in simulation for swarm target scenarios. The impact of two proposed swarm tracking models are compared via Monte Carlo simulation. The focus of these simulations is to evaluate relative performance of the models and not their computational complexity. Design considerations, including uncertainty function design and track feedback hinting that are weighed in single target scenarios are integrated into the swarm tracking case. Each swarm scenario in this section employs a Chi-squared uncertainty function and target track uncertainty feedback as described in section IV.

A. PERFORMANCE METRICS

As in the single target case, target swarm search-and-track performance can be quantified in numerous ways. This section presents the performance metrics used to assess the effectiveness of AB-CRr against various swarm configurations.

1) Swarm Velocity Estimation

One of the core capabilities of swarm target tracking is swarm velocity estimation. In this work, mean swarm velocity estimation is complicated by the radar geometry under investigation. Radar return measurements provide target velocity information relative to the radar receiver (y-axis of the spatial grid), but target motion perpendicular to (x-axis of the spatial grid) the receiver must be estimated from target position history. The responsiveness of swarm tracking models to individual target measurements can be visualized by plotting the mean swarm velocity estimates over time.

2) Swarm Centroid Cost Function

A single target tracking performance cost function can be expressed as

$$\epsilon_c = \frac{1}{N_i}\left(\beta k_0 + \sum_{k=k_0}^{N_i-1} ||\mathbf{x}_k - \hat{\mathbf{x}}_k||_2\right), \tag{43}$$

.

where N is the total number of beam iterations by the radar system, k_0 is the first beam iteration after a target track file has been initialized, and β is a user defined coefficient that weighs the relative contribution of detection latency compared to mean track error. In the swarm tracking case, a tracking cost function can be defined based on the parameters of the target swarm we wish to estimate. Our cost function will seek to minimize the Euclidean distance between the true and estimated swarm mean velocity and spatial centroid, defined previously by the state vector:

This article has been accepted for publication in a future issue of this journal, but has not been fully edited. Content may change prior to final publication. Citation information: DOI 10.1109/ACCESS.2021.3069350, IEEE Access

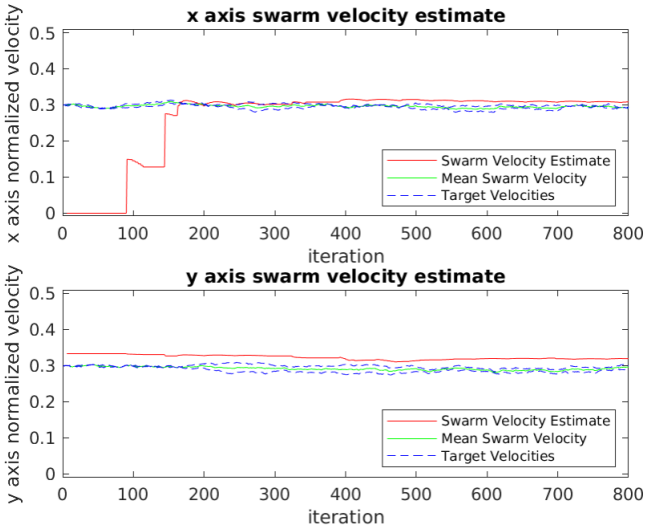

FIGURE 10. Two target swarm mean velocity estimates using separate target track files.

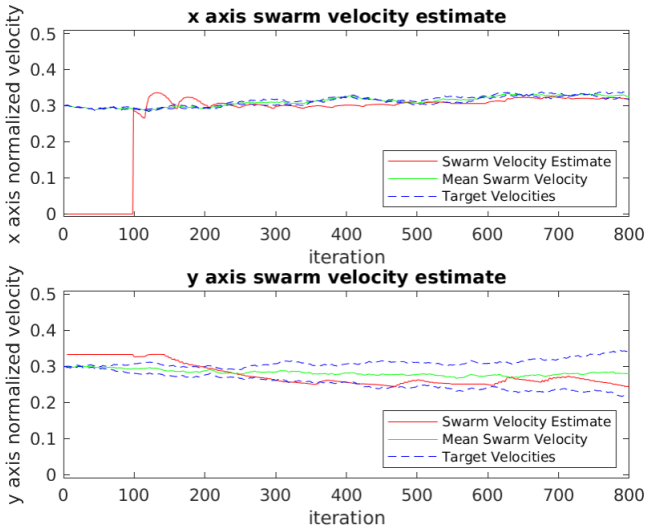

FIGURE 11. Two target swarm mean velocity estimates using a consolidated swarm state vector.

$$\hat{\mathbf{x}}_c = \begin{bmatrix} \mu_x \\ \mu_y \\ \mu_{v_x} \\ \mu_{v_y} \end{bmatrix}. \tag{44}$$

The swarm cost function, or composite centroid error, can then be defined analogously with the single target case:

$$\epsilon_s = \frac{1}{N_i}\left(\beta k_0 + \sum_{k=k_0}^{N_i-1} ||\bar{x}_{c,k} - \hat{x}_{c,k}||_2\right). \tag{45}$$

In this work, β is assumed to be equal to 2.

B. SWARM DETECTION AND TRACKING PERFORMANCE

Two swarm tracking methodologies are compared in this work: using separate individual target track files and a consolidated swarm state vector approach. In this section, we investigate the relative performance of the two methodologies in estimating the mean position and velocity of a target swarm (swarm centroid). All simulations and trials presented are performed via MATLAB with discrete scene dimensions $M_x = M_y = 30$ and $N_y = 9$, for a total of 8100 discrete measurement states. Targets move with a constant average velocity such that they would travel from one edge of the scene to the other edge over the course of 500 radar illuminations. In practice, the actual path of the targets are a variety of diagonal paths, so the targets remain in the scene longer than 500 iterations. However, large deviations to this direction had been tried and were tracked successfully.

1) Two Target Swarm Performance

First, we investigate behavior in a trivial swarm composed of two targets. The mean swarm velocity estimate over the course of a simulation is shown in Fig. 10. In this scenario, a swarm of 2 targets move across the radar search scene in a loose formation with constant mean velocity. The two targets are tracked using separate track files as described in Section IV. The swarm y-axis velocity measurement error is low from the onset of detecting the first target in the swarm. This is expected as y-axis velocity is directly measured by the radar system. The swarm x-axis velocity estimate converges on the swarm true mean velocity more slowly, as the radar system requires multiple track associations to estimate target motion perpendicular to the observer. In the simulation presented, the velocity estimate using the separate track file approach converges to true swarm x-axis velocity in approximately 180 iterations of beam selection (this count is the total number of beam iterations, including iterations that do not illuminate any targets).

Simulating the same scenario with a consolidated swarm track file approach (Fig. 11), we observe a reduction in the number of iterations required for the x-axis velocity estimate to converge on true swarm motion. The consolidated tracking methodology intercepts true swarm x-axis velocity in approximately 100 iterations, compared to 180 iterations with the separate target tracking method. The consolidated track file method outperforms the separate track method in this case because each target association directly updates the velocity estimate, while with the separate target tracking methodology, each individual target track must reach a steady state velocity estimate before the swarm velocity estimate can reach steady state. Additionally, the consolidated swarm tracking model encapsulates targets' spatial correlation in its state estimate covariance matrix $\mathbf{P}$.

Generalizing these observations, the composite swarm tracking error for a two target swarm is estimated via Monte Carlo simulation for both the separate and consolidated tracking models over a range of SNR values. The mean swarm tracking error of 500 iterations of a two target constant

This article has been accepted for publication in a future issue of this journal, but has not been fully edited. Content may change prior to final publication. Citation information: DOI 10.1109/ACCESS.2021.3069350, IEEE Access

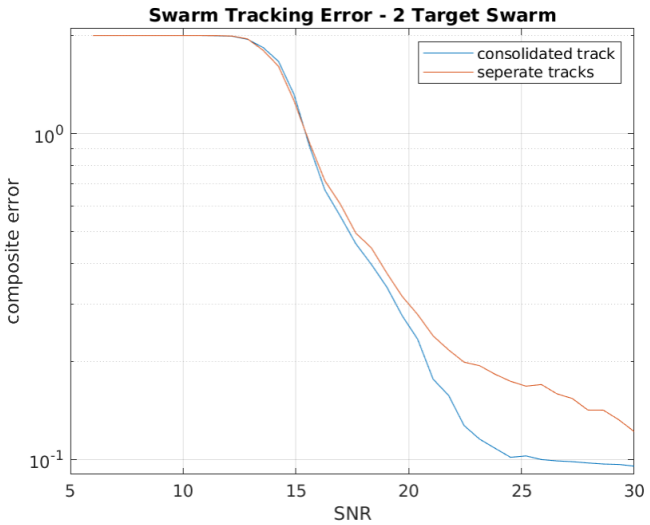

FIGURE 12. Monte Carlo simulation of swarm tracking error for a two target swarm.

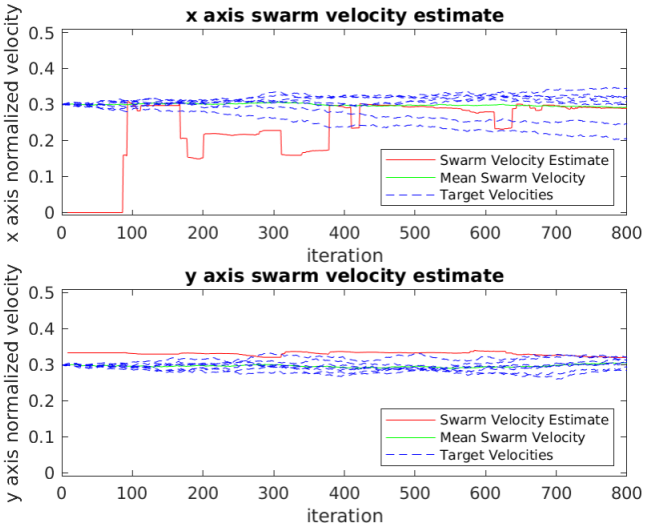

FIGURE 13. Seven target swarm mean velocity estimates using separate target track files.

velocity swarm moving through the search scene is presented in Fig. 12. Note that composite track error (Equation 45) for both a consolidated and separate track methodologies are comparable up to about 16 dB SNR, after which consolidated swarm tracking outperforms individual target track files (we simulated up to 30 dB SNR). At 25 dB SNR, the consolidated tracking method exhibits 38% lower tracking error than the separate tracking counterpart. Therefore, in the trivial two target swarm scenario, consolidated tracking outperforms the individual target tracking method.

2) Seven Target Swarm Performance

Next, we investigate how both swarm tracking methodologies perform when the number of targets in the swarm is increased. Larger swarms present a unique tracking challenge, as beamforming resources are divided among an increasingly

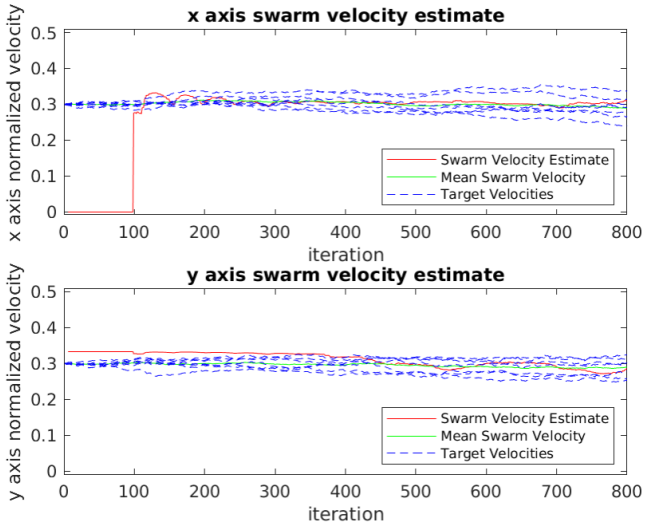

FIGURE 14. Seven target swarm mean velocity estimates using a consolidated swarm state vector.

larger number of target tracks. As a consequence, we expect the swarm tracking error to be higher for a given SNR than in the 2 target case, as beamsteering resources allocated to target tracking will be strained by the large number of targets in the swarm.

Repeating the simulation scenario for Fig. 10 with a seven target swarm and separate target tracking, we see that the swarm x-axis velocity estimate converges slowly towards a steady-state velocity estimate and has a tendency to deviate from the steady state (i.e. an inconsistent estimate). Compared to the two target scenario, which took 100 beam iterations to converge on an x-axis velocity estimate, the seven target scenario estimate (Fig. 13) incrementally reaches true swarm motion but does not maintain that estimate consistently. The AB-CRr system in this scenario is overwhelmed by the number of target tracks to maintain, and poor individual track estimates result in an inconsistent mean swarm velocity estimate.

In comparison, the same seven target swarm scenario tracked with a consolidated swarm state vector achieves much more stable velocity estimates (Fig. 14). This simulated scenario converges to the swarm true x-axis velocity estimate in approximately 100 beam selection iterations. This is similar to the delay of 2 target swarm with consolidated state tracking. As a result, we would expect consolidated swarm tracking to be more robust to large target swarms than the separate target tracking methodology.

The composite swarm tracking error for the seven target swarm is again estimated via Monte Carlo simulation for both the separate and consolidated tracking approaches over a range of SNR, as with the two target scenario. Our results are based on 500 Monte Carlo trials for each environmental noise and tracking method case and are summarized in Fig. 15. Consolidated swarm tracking and individual target tracking have comparable tracking error up to about 18 dB SNR,

This article has been accepted for publication in a future issue of this journal, but has not been fully edited. Content may change prior to final publication. Citation information: DOI 10.1109/ACCESS.2021.3069350, IEEE Access

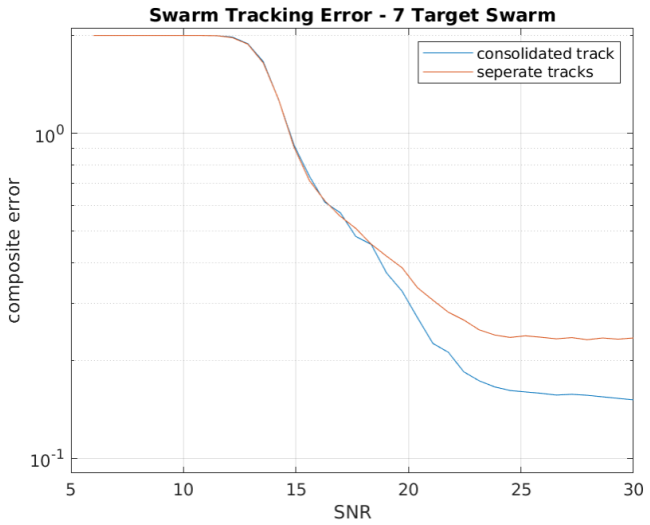

FIGURE 15. Monte Carlo simulation of swarm tracking error for a seven target swarm.

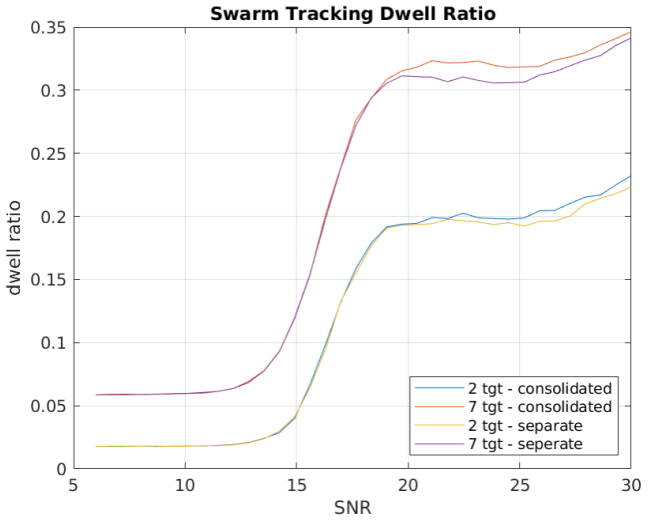

FIGURE 16. Monte Carlo simulation of swarm tracking dwell ratio for various swarm configurations.

after which the consolidated tracking model outperforms the separate target tracks. Both tracking methodologies approach an asymptotic track error between 25 and 30 dB SNR, where composite tracking maintains approximately 34% lower track error than the individual target tracking method.

C. SWARM TARGET SEARCH/TRACKING RESOURCE ALLOCATION

The percentage of time that the radar directs its beam onto active target tracks is referred to here as the dwell ratio, and serves as a metric of detection or search versus tracking resource balancing. A comparison of swarm target tracking dwell ratios for both the consolidated and separate track approaches indicates that the consolidated swarm tracking method does not compromise search/detection performance for its relative improvement in target tracking. Fig. 16 plots the track dwell ratio across a range of SNR for both the 2 target and 7 target swarm scenarios. The consolidated swarm tracking and separate target tracking approaches maintain similar dwell ratios for a given swarm size, indicating that the two methods allocate approximately the same degree of beamsteering resources to swarm tracking.

Therefore, we conclude that consolidated swarm tracking is a more efficient methodology for tracking correlated velocity target swarms than an individual target tracking approach in terms of beamsteering resources.

VI. SUMMARY AND CONCLUSIONS

In this work, we introduced the problem of integrated detection-and-tracking of swarm targets using adaptive beamsteering cognitive radar (AB-CRr) and made multiple contributions which we summarize here. We examined design considerations of a cognitive radar system and how they pertain to beamsteering behavior against groups of targets with correlated motion. Following from prior art, we implemented beamsteering resource allocation between integrated search and tracking applications via a parameterized uncertainty function, settling on a modified Chi-squared uncertainty function for swarm search/detection and tracking. We also introduced an improved uncertainty growth model for updating the target environment probability map compared to prior work. Additionally, this work introduced target track uncertainty feedback and an improved uncertainty growth model into the AB-CRr framework to complement uncertainty function design in modulating beam allocation behavior. As a result, we demonstrated improved beamsteering resource efficiency for search and tracking applications compared to prior AB-CRr configurations.

The use of AB-CRr was then extended to multiple target swarm scenarios. Target swarms were defined as groups of targets with correlated motion. Mahalanobis distance nearest neighbors track association was employed in the swarm target scenario to integrate with Kalman tracking information. Two methodologies were proposed for swarm tracking applications. The first method established an individual Kalman track file for each detected member target of the swarm in the search scene. The second method assumed that each swarm member had the same mean velocity and tracks each member target within the same consolidated swarm state vector. The second methodology took advantage of state correlation between each member target of the swarm.

The performance of both the separate target tracking and consolidated swarm tracking methodologies were evaluated via Monte Carlo simulation. The consolidated swarm tracking methodology outperformed the separate track methodology across a range of SNR and swarm sizes. When target swarms were large, the separate target tracking method exhibited signs of target saturation and resource overloading, while the consolidated swarm tracking method maintained up

to 34% lower composite swarm tracking error in high SNR conditions.

Overall, AB-CRr presents a promising approach to improving beamsteering resource efficiency in the presence of large swarm targets. An AB-CRr framework tailored to robust tracking of a large number of swarm targets is presented in this work, employing a parameterized uncertainty function, swarm target feedback to the beamsteering uncertainty model, and a consolidated swarm state vector approach to Kalman filter target tracking.

REFERENCES

[1] L. A. Boggio and D. R. Fuhrmann, "Active-testing surveillance for multiple target detection with composite hypotheses," in *IEEE Workshop on Statistical Signal Processing, 2003*, pp. 641-644, 2003.

[2] N. A. Goodman, P. R. Venkata, and M. A. Neifeld, "Adaptive waveform design and sequential hypothesis testing for target recognition with active sensors," *IEEE Journal of Selected Topics in Signal Processing*, vol. 1, no. 1, pp. 105-113, 2007.

[3] R. Romero and N. A. Goodman, "Improved waveform design for target recognition with multiple transmissions," in *2009 International Waveform Diversity and Design Conference*, pp. 26-30, 2009.

[4] S. Haykin, "Cognitive radar: a way of the future," *IEEE Signal Processing Magazine*, vol. 23, no. 1, pp. 30-40, 2006.

[5] H.-S. Kim, N.A. Goodman, C.K. Lee, S.-I. Yang, "Improved waveform design for radar target classification", *Electronics Letters*, vol. 53, no. 13, pp. 879-881, 2017.

[6] Peng Chen, Lenan Wu, "Waveform design for multiple extended targets in temporally correlated cognitive radar system", *Radar Sonar Navigation IET*, vol. 10, no. 2, pp. 398-410, 2016.

[7] Xiaowen Zhang, Kaizhi Wang, Xingzhao Liu, "Joint optimisation of transmit waveform and receive filter for cognitive radar", *Radar Sonar Navigation IET*, vol. 12, no. 1, pp. 11-20, 2018.

[8] Gaia Rossetti, Sangarapillai Lambotharan, "Robust Waveform Design for Multistatic Cognitive Radars", *Access IEEE*, vol. 6, pp. 7464-7475, 2018.

[9] Hui Sheng, Kaizhi Wang, Xingzhao Liu, "Optimum two-dimensional transmit-receiver design", *Geoscience and Remote Sensing Symposium (IGARSS) 2012 IEEE International*, pp. 4610-4613, 2012.

[10] Xiaowen Zhang, Kaizhi Wang, Yesheng Gao, Xingzhao Liu, "Optimal waveform design oriented toward cognitive radar in fractional Fourier domain", *Radar Conference (RadarConf) 2016 IEEE*, pp. 1-5, 2016.

[11] Wang Kaizhi, Liu Xingzhao, "Cognitive SAR based on waveform design and optimum", *Waveform Diversity Design Conference (WDD) 2012 International*, pp. 256-259, 2012.

[12] Yujie Gu, Nathan A. Goodman, "Information-Theoretic Waveform Design for Gaussian Mixture Radar Target Profiling", *Aerospace and Electronic Systems IEEE Transactions on*, vol. 55, no. 3, pp. 1528-1536, 2019.

[13] L.K. Patton, S.W. Frost, B.D. Rigling, "Efficient design of radar waveforms for optimised detection in coloured noise", *IET Radar, Sonar Navigation*, vol. 6, pp. 21, 2012.

[14] Qinling Jeanette Olivia Tan, Ric A. Romero, "Ground vehicle target signature identification with cognitive automotive radar using 24–25 and 76–77GHz bands", *IET Radar, Sonar, and Navigation*, 2018.

[15] Kang Li, Bo Jiu, Hongwei Liu, Siyuan Liang, "Waveform design for cognitive radar in presence of jammer using Stackelberg game", *The Journal of Engineering*, 2019.

[16] Jo-Yen Nieh, Ric A. Romero, "Comparison of ambiguity function of eigenwaveform to wideband and pulsed radar waveforms: a comprehensive tutorial", *Journal of Engineering The*, vol. 2018, no. 4, pp. 203-221, 2018.

[17] R. A. Romero, J. Bae and N. A. Goodman, "Theory and Application of SNR and Mutual Information Matched Illumination Waveforms," in *IEEE Transactions on Aerospace and Electronic Systems*, vol. 47, no. 2, pp. 912-927, April 2011.

[18] W. Yi, Y. Yuan, R. Hoseinnezhad and L. Kong, "Resource Scheduling for Distributed Multi-Target Tracking in Netted Colocated MIMO Radar Systems," in *IEEE Transactions on Signal Processing, vol. 68*, pp. 1602-1617, 2020.

[19] J. Yan, W. Pu, J. Dai, H. Liu and Z. Bao, "Resource Allocation for Search and Track Application in Phased Array Radar Based on Pareto Bi-Objective Optimization," in *IEEE Transactions on Vehicular Technology, vol. 68, no. 4*, pp. 3487-3499, April 2019.

[20] Stefan Brüggenwirth, Marcel Warnke, Simon Wagner, Kilian Barth, "Cognitive Radar for Classification", *Aerospace and Electronic Systems Magazine IEEE*, vol. 34, no. 12, pp. 30-38, 2019.

[21] P. Nielsen and N. A. Goodman, "Integrated detection and tracking via closed-loop radar with spatial-domain matched illumination," in *2008 International Conference on Radar*, pp. 546-551, Sep. 2008.

[22] R. Romero, "Matched waveform design and adaptive beamsteering in cognitive radar applications," Ph.D. dissertation, University of Arizona, 2010.

[23] K. L. Bell, C. J. Baker, G.E. Smith, J.T. Johnson, and M. Rangaswamy, "Cognitive radar framework for target detection and tracking," *IEEE Journal of Selected Topics in Signal Processing*, vol. 9, no. 8, Dec. 2015, pp. 1427-1439.

[24] A. E. Mitchell, G. E. Smith, K. L. Bell, A. Duly, and M. Rangaswamy, "Fully adaptive radar cost function design," in *2018 IEEE Radar Conference (RadarConf18)*, 2018, pp. 1301-1306.

[25] R. A. Romero and N. A. Goodman, "Cognitive radar network: Cooperative adaptive beamsteering for integrated search-and-track application," *IEEE Transactions on Aerospace and Electronic Systems*, vol. 49, no. 2, April 2013, pp. 915-931.

[26] Z. W. Johnson and R. A. Romero, "Uncertainty function design for adaptive beamsteering cognitive radar," in *2020 IEEE International Radar Conference (RADAR)*, April 2020, pp. 1058-1062.

[27] R. A. Romero, C. M. Kenyon, and N. A. Goodman, "Channel probability ensemble update for multiplatform radar systems," in *2010 International Waveform Diversity and Design Conference*, Aug. 2010, pp. 182-187.

[28] R. A. Romero and N. A. Goodman, "Adaptive beamsteering for search-and-track applications with cognitive radar network," in *2011 IEEE RadarCon (RADAR)*, pp. 1091-1095, May 2011.

[29] Q. Huang, D. Lu, L. He, R. Zhan and J. Zhang, "Group Tracking Method with Adaptive Gate for Multiple Extended Objects Tracking", 2019 IEEE 4th International Conference on Signal and Image Processing (ICSIP), Wuxi, China, 2019, pp. 773-776, doi: 10.1109/SIPROCESS.2019.8868590.

[30] S. Yang, K. Thormann and M. Baum, "Linear-Time Joint Probabilistic Data Association for Multiple Extended Object Tracking," 2018 IEEE 10th Sensor Array and Multichannel Signal Processing Workshop (SAM), Sheffield, UK, 2018, pp. 6-10, doi: 10.1109/SAM.2018.8448430.

[31] L. A. Giefer, J. Clemens and K. Schill, "Extended Object Tracking on the Affine Group Aff (2)," 2020 IEEE 23rd International Conference on Information Fusion (FUSION), Rustenburg, South Africa, 2020, pp. 1-8, doi: 10.23919/FUSION45008.2020.9190566.

[32] J. Lan and X. R. Li, "Extended-Object or Group-Target Tracking Using Random Matrix With Nonlinear Measurements," in IEEE Transactions on Signal Processing, vol. 67, no. 19, pp. 5130-5142, 1 Oct.1, 2019, doi: 10.1109/TSP.2019.2935866.

[33] M. Schuster, J. Reuter and G. Wanielik, "Multi detection joint integrated probabilistic data association using random matrices with applications to radar-based multi object tracking", J. Adv. Inf. Fusion, vol. 12, no. 2, pp. 175-188, 2017.

[34] W. Aftab, R. Hostettler, A. De Freitas, M. Arvaneh and L. Mihaylova, "Spatio-Temporal Gaussian Process Models for Extended and Group Object Tracking With Irregular Shapes," in IEEE Transactions on Vehicular Technology, vol. 68, no. 3, pp. 2137-2151, March 2019, doi: 10.1109/TVT.2019.2891006.

[35] P. M. Siew, R. Linares and V. L. Bageshwar, "Extended Target Tracking and Shape Estimation via Random Finite Sets," 2019 American Control Conference (ACC), Philadelphia, PA, USA, 2019, pp. 5346-5351, doi: 10.23919/ACC.2019.8814587.

[36] A. S. Rahmathullah, Á. F. García-Fernández and L. Svensson, "Generalized optimal sub-pattern assignment metric," 2017 20th International Conference on Information Fusion (Fusion), Xi'an, China, 2017, pp. 1-8, doi: 10.23919/ICIF.2017.8009645.

[37] B. M. Bey, "Clutter covariance modelling matlab code," August 2019, unpublished.

[38] W. MathWorld. Binomial series. [Online]. Available: http://mathworld.wolfram.com/BinomialSeries.html

[39] S. S. Skiena, *The Algorithm Design Manual*. Springer, 2010.

This article has been accepted for publication in a future issue of this journal, but has not been fully edited. Content may change prior to final publication. Citation information: DOI 10.1109/ACCESS.2021.3069350, IEEE Access

ZACHARY W. JOHNSON (S'18) received the B.S.E.E degree from the US Naval Academy, Annapolis, MD, USA, in 2019, and the M.S.E.E degree from the Naval Postgraduate School, Monterey, CA, USA, in 2020.

He was a Bowman Research Scholar at the US Naval Academy and was involved in research related to embedded systems security and forensics. His research interests include adaptive control systems, signal processing, and RF technologies.

Mr. Johnson was awarded the 2020 Naval Information Warfare Systems Command Award in Electronic Systems Engineering at the Naval Postgraduate School.

RIC A. ROMERO (S'07-M'10-SM'12) received the B.S.E.E degree from Purdue University, West Lafayette, IN, USA, in 1999, the M.S.E.E degree from the University of Southern California, Los Angeles, CA, USA, in 2004, and the Ph.D. degree in electrical and computer engineering from The University of Arizona, Tucson, AZ, USA, in 2010.

He was a Senior Multidisciplined Engineer II with Raytheon Missile Systems, Tucson, from 1999 to 2010. He was involved in various communications, radar, and research and development programs. He was also a Graduate Research Assistant with the Laboratory for Sensor and Array Processing, The University of Arizona, from 2007 to 2010. He is currently an Associate Professor with the Department of Electrical and Computer Engineering, Naval Postgraduate School, Monterey, CA, USA. His research interests include the general areas of radar, sensor information processing, and communications.

Dr. Romero was awarded the 2004 Corporate Excellence in Technology Award, which is a company-wide technical prize at Raytheon Corporation. He was also granted the Raytheon Advanced Scholarship Program Fellowships, from 2002 to 2004 and from 2005 to 2007.